

**ROSUVASTATIN ATTENUATES HYPERTENSION-INDUCED  
CARDIOVASCULAR REMODELLING WITHOUT AFFECTING BLOOD  
PRESSURE IN DOCA-SALT HYPERTENSIVE RATS**

David Loch<sup>1</sup>, Scott Levick<sup>1</sup>, Andrew Hoey<sup>2</sup> and Lindsay Brown<sup>1</sup>

1 Department of Physiology and Pharmacology, School of Biomedical Sciences,  
The University of Queensland 4072, AUSTRALIA

2 Centre for Biomedical Research, Faculty of Sciences, University of Southern  
Queensland, Toowoomba 4350, AUSTRALIA

*Address for Correspondence:*

Assoc Prof Lindsay Brown, Department of Physiology and Pharmacology, School of  
Biomedical Sciences, The University of Queensland 4072, AUSTRALIA; telephone +61  
7 3365 3098; fax +61 7 3365 1766; email [l.brown@uq.edu.au](mailto:l.brown@uq.edu.au)

*Short Title:*

Rosuvastatin and remodelling in DOCA-salt rats

*Sources of Support:*

This study was supported in part by a grant from AstraZeneca, Macclesfield, Cheshire  
U.K.

## **ABSTRACT**

The pleiotropic effects of statins represent potential mechanisms for the treatment of end-organ damage in hypertension. This study has investigated the effects of rosuvastatin in a model of cardiovascular remodelling, the DOCA-salt hypertensive rat. Male Wistar rats weighing 300-330g were uninephrectomized (UNX) or uninephrectomized and treated with DOCA (25 mg subcutaneously every fourth day) and 1% NaCl in the drinking water. Compared with UNX controls, DOCA-salt rats developed hypertension, cardiovascular hypertrophy, inflammation with perivascular and interstitial cardiac fibrosis, endothelial dysfunction and prolongation of ventricular action potential duration at 28 days. Rosuvastatin treated rats received 20mg/kg/day of the drug in 10% Tween 20 by oral gavage for 32 days commencing 4 days before uninephrectomy. UNX and DOCA-salt controls received vehicle only. Rosuvastatin therapy attenuated the development of cardiovascular hypertrophy, inflammation, fibrosis and ventricular action potential prolongation, but did not modify hypertension or vascular dysfunction. We conclude that the pleiotropic effects of rosuvastatin include attenuation of aspects of cardiovascular remodelling in the DOCA-salt model of hypertension in rats without altering systolic blood pressure.

**Key Terms: DOCA-salt rat; Rosuvastatin; Hypertension; Fibrosis; Hypertrophy.**

## **INTRODUCTION**

Although many drugs efficiently lower serum cholesterol levels, none have been more successful and well tolerated than the 3-hydroxy-3-methylglutaryl coenzyme A (HMG-CoA) reductase inhibitors. The statins, as they are more commonly known, reduce cardiovascular mortality in primary and secondary prevention trials of coronary heart disease in patients with high or moderate hypercholesterolaemia [1-5] and even normal cholesterol levels [1, 5, 6]. This clinical benefit of statins may occur relatively early after initiation of therapy [3-5] and before any regression in atherosclerotic plaques can be detected [7]. In addition, their effects differ from those observed after the reduction of plasma cholesterol levels by surgical therapy [8]. These findings suggest that statins work by mechanisms additional to a decrement in plasma lipid concentrations and atherosclerotic plaque prevention or regression. Such pleiotropic effects include inhibiting the thrombogenic response and reducing oxidative stress and inflammation [9].

More recently, several studies have documented that the pleiotropic effects of statins extend to the prevention of pathological cardiovascular remodelling in animal models of human disease, such as rat models of post-infarct heart failure [10] and type II diabetes mellitus [11]. However, it is unclear whether these cardioprotective effects are shared by all statins. This is especially important, considering the highly varied chemical structures, physicochemical and pharmacokinetic/metabolic properties of the many members of the statin family [12, 13] and the documented differences not only in their lipid lowering potential, but also in their nonlipid effects, particularly cardiovascular hypertrophy [14-16].

Rosuvastatin is a new synthetic and chemically distinct member of the statin family [13]. Clinical evidence has shown that rosuvastatin is the most effective statin with regards to lipid lowering [17]. However, whether rosuvastatin possesses the ability to exert similar, or more significant, beneficial effects on cardiovascular remodelling is yet to be established. There have been a number of publications showing rosuvastatin to be protective in cardiac ischemia-reperfusion injury models [18-20]. Consequently, we have investigated the potential pleiotropic effects of rosuvastatin on cardiovascular remodelling in the DOCA-salt model of hypertension in rats.

## **METHODS**

### ***Ethical Clearance***

All experimentation was approved by the Animal Experimentation Ethics Committee of The University of Queensland under the guidelines of the National Health and Medical Research Council of Australia.

### ***DOCA-salt hypertensive rats***

Male Wistar rats weighing 300-330g (~8 weeks old) were obtained from the Central Animal Breeding House of The University of Queensland. All rats were uninephrectomized. This was done under anaesthesia with intraperitoneal tiletamine (25 mg/kg) and zolazepam (25 mg/kg)(Zoletil®) combined with xylazine (10 mg/kg)(Ilium Xylazil®). Kidneys were visualised by a left lateral abdominal incision. The left kidney was removed after ligation of adjoining renal vasculature and ureter with sutures. The

capsule was removed from the left kidney, which was then weighed. Uninephrectomized rats were given either no further treatment (UNX rats) or 1% NaCl in the drinking water with subcutaneous injections of deoxycorticosterone acetate (DOCA; 25mg in 0.4ml dimethylformamide every fourth day) (DOCA-salt rats). Rosuvastatin-treatment groups received 20mg/kg/day rosuvastatin in 10% Tween 20 by oral gavage for 32 days commencing 4 days before uninephrectomy. UNX and DOCA-salt controls received vehicle only. Experiments were performed 28 days after surgery.

### ***Assessment of Physiological Parameters***

Systolic blood pressure was measured by tail-cuff plethysmography in rats lightly anaesthetised with intraperitoneal tiletamine (10 mg/kg) and zolazepam (10 mg/kg). Rats were euthanased with pentobarbitone (200 mg/kg ip). Blood was taken from the abdominal vena cava, just caudal to the insertion of renal veins, centrifuged and the plasma immediately frozen. Plasma sodium and potassium concentrations were measured by flame photometry. The heart was removed and weighed immediately after death and expressed as a ratio of the tissue weight (mg) to the total body weight (g). Plasma levels of total cholesterol were measured by The University of Queensland Veterinary Pathology Services, Brisbane, Australia.

### ***Isolated Langendorff heart preparation***

Rats were anaesthetized with sodium pentobarbitone (100 mg/kg ip) and heparin (200 IU) was administered via the femoral vein. After allowing two minutes for the heparin to circulate, the heart was excised and placed in cooled (0°C) crystalloid perfusate (modified

Krebs-Henseleit solution of the following composition in mM: NaCl 119.1, KCl 4.75, MgSO<sub>4</sub> 1.19, KH<sub>2</sub>PO<sub>4</sub> 1.19, CaCl<sub>2</sub> 2.16, NaHCO<sub>3</sub> 25.0, glucose 11.0). A cannula was then placed in the heart with its tip immediately above the coronary ostia of the aortic stump. The cannula was used to perfuse the heart in a non-recirculating Langendorff fashion at 100cm of hydrostatic pressure. The perfusate temperature was maintained at 37°C and bubbled with 95%O<sub>2</sub> / 5%CO<sub>2</sub>. The apex of the heart was pierced to facilitate thebesian drainage and paced at 250 bpm.

Left ventricular developed pressure was measured using a balloon catheter inserted into the left ventricle through the mitral orifice. The catheter was connected via a three-way tap to a micrometer syringe and to a MLT844 Physiological Pressure Transducer (ADInstruments) and PowerLab data acquisition unit (ADInstruments). The outer diameter of the catheter was similar to the mitral annulus to prevent ejection of the balloon during the systolic phase. After a 5-minute stabilization period, steady-state left ventricular pressure was recorded from isovolumetrically beating hearts. Increments in balloon volume were applied to the heart with left ventricular end-diastolic pressure recorded at approximately 0, 5, 10, 15, 20 and 30mmHg. At the end of the experiment, the atria and right ventricle were dissected away leaving the left ventricle and septum, which were blotted dry then weighed.

Myocardial diastolic stiffness was calculated as the diastolic stiffness constant ( $k$ , dimensionless), the slope of the linear relation between tangent elastic modulus ( $E$ , dyne/cm<sup>2</sup>) and stress ( $\sigma$ , dyne/cm<sup>2</sup>) [21].

### ***Isolated thoracic aortic rings***

Thoracic aortic rings (approximately 4 mm in length) were suspended with a resting tension of 10 mN. Cumulative concentration-response curves were performed for noradrenaline and either acetylcholine or sodium nitroprusside in the presence of a submaximal (~70%) contraction to noradrenaline.

### ***Quantification of Left Ventricular Collagen***

Collagen content was determined by image analysis of picrosirius red-stained sections of the hearts [22]. In brief, transverse sections were stored initially in Telly's fixative (100mL 70% ethanol; 5mL glacial acetic acid; 10mL formaldehyde) for 3 days, then transferred to modified Bouin's solution (85 mL saturated picric acid; 5 mL glacial acetic acid; 10 mL 40% formaldehyde) for two days and then stored in 70% ethanol.

Sections were subsequently embedded in wax and sliced into 10  $\mu$ m sections. These were stained with picrosirius red (0.1% Sirius Red F3BA in picric acid). Slides were left in 0.2% phosphomolybdic acid for 5 minutes, washed, left in picrosirius red for 90 minutes, then in 1 mM HCl for 2 minutes and 70% ethanol for 45 seconds. The stained sections were mounted with Depex and visualized using a Biorad MRC-1024 confocal laser-scanning microscope with a Red/Texas Red filter with excitation at 568 nm and green emission at 609 nm. Images were acquired with an objective lens of 40x magnification and quantified using NIH-image software (National Institute of Health, USA). At least 4

areas from each heart were analysed and collagen levels expressed as a percentage of red area in each image.

Histological collagen results were confirmed by hydroxyproline assay adapted from Stegemann and Stalder [23]. Approximately 2.5 and 5.0 mg samples of thoracic aorta and left ventricle respectively were dried for 6 hours at 40°C. Tissues and standards were then hydrolyzed in 6N HCl at 107°C for 18 hours. The acid was blown off by compressed air and the hydrolysate reconstituted in distilled water. Chloramine T reagent was added to each sample for the oxidation step to progress, followed by Ehrlich's reagent to enable chromophore development. Absorbance of each sample was read at 550nm in a spectrophotometer and hydroxyproline content established from a standard curve.

#### ***Width of Media in Thoracic Aorta***

The width of the media in the thoracic aorta of rats was measured by image analysis of picosirius red-stained sections. Section preparation, staining, image acquisition and analysis were similar to those mentioned above. Three different areas of each aorta were measured and the results averaged.

#### ***Immunofluorescence of ED-1 positive cells in the Left Ventricle***

Briefly, 5 µm thick sections were initially incubated with primary antibodies for rat macrophages (ED1; Serotec mouse anti-rat ED1 diluted 1:15). Omission of primary antibodies, and staining with an irrelevant mouse immunoglobulin of the same isotype, served as negative controls. Samples were then incubated with IgG-fluorescein

conjugated secondary antibody (Chemicon; diluted 1:200). Sections were counterstained with propidium iodide, mounted and visualized with a confocal laser-scanning microscope. A zero to four grading scale was used to classify the extent of ED-1 positive monocyte/macrophage infiltration in the left ventricle. 0 = no inflammatory cells present; 1 = low level of inflammatory cells throughout the left ventricle; 2 = moderate levels of inflammatory cells throughout the left ventricle and concentrated in mild scarring; 3 = high levels of inflammatory cells throughout the left ventricle and concentrated in moderate scarring; 4 = high levels of inflammatory cells throughout the left ventricle and concentrated in heavy scarring.

#### ***Microelectrode studies of isolated left ventricular papillary muscles***

Electrophysiological recordings of cardiac action potentials were obtained by microelectrode single cell impalements of *ex vivo* left ventricular papillary muscles. Rats were euthanased by carbon dioxide inhalation with subsequent exsanguination. The heart was removed and placed in chilled Tyrode's physiological salt solution (in mM: NaCl 136.9, KCl 5.4, MgCl<sub>2</sub>.H<sub>2</sub>O 1.0, NaH<sub>2</sub>PO<sub>4</sub>.2H<sub>2</sub>O 0.4, NaHCO<sub>3</sub> 22.6, CaCl<sub>2</sub>.2H<sub>2</sub>O 1.8, glucose 5.5, ascorbic acid 0.3, Na<sub>2</sub>-EDTA 0.05) bubbled with 95% O<sub>2</sub> / 5% CO<sub>2</sub>, where the left ventricular papillary muscles were promptly dissected out. A stainless steel hook was placed through the valvular end of the papillary muscle, and a 30G needle was used to fix the apical end. The needle was subsequently embedded into a rubber base placed in a 1.0mL experimental chamber continuously perfused with carbogenated, warm (35±0.5°C) Tyrode's solution at ~3 mL/min. The hook was attached to a modified sensor element (Sensonor AE801) connected to an amplifier (World Precision Instruments,

TBM-4). The muscle was stretched slowly to the required preload (3-5mN). Papillary contractions were induced by field stimulation (Grass SD-9) via electrodes on each side of the muscle (stimulation frequency 1 Hz; pulse width 0.5 ms; stimulus strength 20% above threshold).

The muscle was allowed to equilibrate for 30 minutes then impaled with a microelectrode (World Precision Instruments, filamented borosilicate glass, outer diameter 1.5 mm) with a tip resistance of 5-15 M $\Omega$  when filled with 3M KCl. Perfusion and recording then continued for another 30 minutes. Action potential parameters measured were action potential duration (APD) at 20%, 50% and 90% of repolarization (APD<sub>20</sub>, ADP<sub>50</sub> and APD<sub>90</sub> respectively), action potential amplitude and resting membrane voltage. The reference electrode was a Ag/AgCl electrode. A Cyto 721 electrometer (World Precision Instruments) was used to record bioelectrical activity. All signals were recorded via a PowerLab 4S data acquisition unit (ADInstruments). Data were acquired, derived and analysed using Chart 4.3 software (ADInstruments).

### ***Data analysis***

All results are given as mean  $\pm$  SEM. The negative log EC<sub>50</sub> of the increase in force of contraction in mN was determined from the concentration giving half-maximal responses in individual concentration-response curves. These results were analysed by one-way analysis of variance followed by the Bonferroni post test to determine differences between treatment groups; p<0.05 was considered significant.

## *Drugs*

Deoxycorticosterone acetate, acetylcholine, sodium nitroprusside and noradrenaline were purchased from Sigma Chemical Company, St Louis, MO, USA. Rosuvastatin calcium was provided by AstraZeneca, U.K.. Noradrenaline, sodium nitroprusside and acetylcholine were dissolved in distilled water; deoxycorticosterone acetate was dissolved in dimethylformamide with mild heating.

## **RESULTS**

Control and rosuvastatin-treated UNX rats gained similar weight over the 4 week protocol. Both DOCA-salt groups, on the other hand, failed to gain body weight in this period (Table 1). The systolic blood pressure of DOCA-salt rats rose significantly at 2 weeks and even further at 4 weeks (Table 1). Rosuvastatin treatment had no effect on this developing hypertension in DOCA-salt rats. UNX rats exhibited no alterations in blood pressure (Table 1). Total plasma cholesterol concentration was significantly augmented in DOCA-salt rats, while rosuvastatin treatment normalized this parameter in these rats (Table 1). The concentration of plasma sodium was unaltered amongst the four rat groups; however, plasma potassium concentration was decreased in both control and treatment DOCA-salt groups (Table 1).

DOCA-salt animals exhibited an increase in left ventricular mass that was attenuated by rosuvastatin treatment (Table 1). Fibrosis following an increased infiltration of inflammatory cells is characteristic of the DOCA-salt rat left ventricle [24]. We have shown that the left ventricular tissue of DOCA-salt animals exhibited considerable ED1-

positive inflammatory cell infiltration compared to UNX controls, and this inflammation was prevented by rosuvastatin (Figure 2). The left ventricular tissue of DOCA-salt control rats was also found to be substantially fibrosed, as evidenced by a significant increase in both interstitial and perivascular left ventricular collagen area compared with UNX controls (Figure 1). Rosuvastatin treatment was successful in attenuating the increase in interstitial collagen area (Figure 1). The drug also normalized the perivascular collagen area of DOCA-salt rats (Figure 1). An alternative measure of cardiac fibrosis, hydroxyproline content, was also elevated in the left ventricle of DOCA-salt control rats in comparison to UNX animals (Figure 1). Once again, rosuvastatin treatment reduced this indicator of cardiac fibrosis (Figure 1). The isolated perfused hearts of DOCA-salt control rats exhibited an increased diastolic stiffness constant compared to UNX animals. Rosuvastatin treatment of these animals normalized this measure of cardiac stiffness (Table 1).

Electrophysiological studies of isolated papillary muscles revealed no difference in resting membrane potential and action potential amplitude between UNX and DOCA-salt rats (Table 2). DOCA-salt rats showed significant electrical remodelling, manifested as prolonged action potential durations at 20%, 50% and 90% of repolarization ( $APD_{20}$ ,  $APD_{50}$  and  $APD_{90}$ ) (Table 2, Figure 4). Rosuvastatin treatment significantly attenuated this prolongation of  $APD_{90}$ , but not  $APD_{20}$  or  $APD_{50}$  (Table 2, Figure 4).

The thoracic aorta media width of DOCA-salt rats was found to be significantly increased compared to UNX rats, with rosuvastatin therapy attenuating this vascular hypertrophy

(Table 1). In contrast, the hydroxyproline content of these vessels was similar among groups (Table 1). Vascular smooth muscle dysfunction was evidenced by the reduced contractile response to noradrenaline, as well as the decreased relaxant response to sodium nitroprusside in isolated thoracic aortic rings of DOCA-salt rats compared to UNX controls (Figure 3A and C). There was also an increased potency of noradrenaline-induced contraction in these rings (Figure 3A). Relaxant responses to acetylcholine were also reduced in hypertensive rats compared to their normotensive controls (Figure 3B). Rosuvastatin was without effect on these reduced responses to noradrenaline, sodium nitroprusside and acetylcholine in DOCA-salt rats (Figure 3A, B and C). Drug therapy augmented aortic responses to acetylcholine in UNX animals (Figure 3B).

## **DISCUSSION**

Rats represent an excellent model for studying the pleiotropic effects of statins, as their lipid profile has been demonstrated to be refractory to statin therapy [25] and, in comparison to humans, their plasma lipid levels are relatively low. In the current study, we investigated the effects of a new HMG-CoA reductase inhibitor, rosuvastatin, on cardiovascular remodelling in the DOCA-salt model of hypertension in rats. We show for the first time that rosuvastatin attenuated left ventricular fibrosis, hypertrophy, inflammation and action potential prolongation and aortic medial hypertrophy, without antihypertensive action in this rodent model of end-organ damage.

Statins have been reported to reduce blood pressure in a randomized, double-blind crossover trial in humans (pravastatin) [26] and hypertensive rodent models (simvastatin

and lovastatin) [27, 28], including DOCA-salt hypertensive mice (lovastatin) [29]. We, on the other hand, found that rosuvastatin was without effect on DOCA-salt-induced hypertension in rats. This difference may be related to model and species differences or the relative hydrophilicity of rosuvastatin limiting its uptake through their plasma membrane. However, independent of any anti-hypertensive effect, rosuvastatin attenuated the increase in left ventricular mass and medial hypertrophy of the thoracic aorta associated with DOCA-salt treatment. In the genetically hypertensive (GH) rat, fluvastatin had no effect on blood pressure, but significantly remodelled the mesenteric resistance and basilar arteries by reducing medial cross-sectional area and increasing lumen size [30]. Furthermore, long-term administration of simvastatin to rats with aortic stenosis inhibited left ventricular hypertrophy without effect on the elevated carotid mean arterial pressure [31]. Taken together, these data support the notion that a reduction of blood pressure is not the primary factor involved in the inhibitory effect of statins on cardiovascular hypertrophy.

In the current study, rosuvastatin therapy reduced left ventricular monocyte infiltration. Such infiltration has been demonstrated to participate in the initiation and progression of cardiovascular pathology in the DOCA-salt model [24, 32]. HMG-CoA reductase inhibitors modulate several different components of the inflammatory cascade, particularly those involving leucocyte-endothelium interactions, such as the down regulation of cell adhesion molecule expression [9]. Indeed, rosuvastatin inhibited endothelial cell surface expression of the adhesion molecule P-selectin, and thus

attenuated leukocyte rolling, adherence and transmigration in normocholesterolaemic rat mesenteric venules [33].

Inflammation has also been shown to play a role in long-term pathological cardiovascular changes, such as matrix accumulation [34]. Hence the anti-fibrotic properties of rosuvastatin in DOCA-salt rats, manifest as reduced LV collagen and hydroxyproline contents and diastolic stiffness (an indirect measure of total collagen), may in part be due to a direct inhibitory effect of the drug upon monocyte/macrophage infiltration. This is supported by Ammarguella and co-workers [24], who have identified inflammatory mediators as a major component of cardiac remodelling and critical to the progression of cardiac fibrosis in this model of mineralocorticoid-induced hypertension. Furthermore, Kagitani *et al.* [32] showed that tranilast, an anti-inflammatory drug, suppressed myocardial fibrosis via inhibition of cytokines, such as monocyte chemoattractant protein-1 and interleukin-6, and monocyte/macrophage infiltration in DOCA-salt rats. Taken together, these results suggest that pharmacological attenuation of the inflammatory response by rosuvastatin may, in part, be responsible for preventing myocardial fibrosis in DOCA-salt rats. This effect may also potentially translate to fibrosis-associated abnormalities, such as diastolic stiffness. Our previous studies with L-arginine, the NO precursor, and A-127722, a selective ET<sub>A</sub>-receptor antagonist, have shown attenuation of inflammatory cell infiltration, myocardial collagen deposition and diastolic stiffness [35, 36].

Action potential prolongation is a common electrophysiological disturbance in hypertrophied myocardium [37] and this includes DOCA-salt animals [38]. We show an approximate 2-fold increase in APD<sub>90</sub> as a result of mineralocorticoid and salt treatment. It appears that depression of the calcium-independent transient outward K<sup>+</sup> current (I<sub>t0</sub>) is responsible for the majority of this prolongation observed in DOCA-salt ventricular myocytes; an absence of enhanced I<sub>t0</sub> channel expression concurrent with hypertrophy resulted in a reduced channel density per unit surface area [38]. Furthermore, regression of LV hypertrophy in DOCA-salt rats normalized the I<sub>t0</sub> current and APD [38]. Thus, the observed attenuation of cardiac action potential prolongation by rosuvastatin is most likely secondary to its amelioration of left ventricular hypertrophy in these rats. This is supported by recent work from our laboratory demonstrating improvement in cardiac action potential prolongation in association with pharmacologic-induced regression of left ventricular hypertrophy in DOCA-salt rats [35, 36].

Hypercholesterolaemia has been shown to induce endothelial dysfunction, an attribute of the initial stages of atherosclerosis [39]. It is not surprising then that statins have been shown to be useful in the reversal of endothelial dysfunction, as documented with non-invasive techniques [40-42]. This effect, however, may also be partly independent of a reduction in cholesterol levels [41]. Nonetheless, DOCA-salt rats develop endothelial dysfunction because of severe hypertension, rather than lipid disorders. In the current study, rosuvastatin was without effect on endothelial dysfunction in DOCA-salt animals. This may be attributed to species differences and variation in the capacity of statins to penetrate vascular cell membranes, but it is also conceivable that blood pressure lowering

may be a prerequisite for the improvement of endothelial dysfunction in DOCA-salt hypertension. However, it is difficult to make a clear distinction on this anomaly, as a result of the reduced relaxant response to sodium nitroprusside, as well as noradrenaline, in DOCA-salt rats, indicating a primary dysfunction of vascular smooth muscle. Rosuvastatin did, however, improve endothelium-dependent acetylcholine-induced vascular relaxations in normotensive UNX rats.

The exact mechanism by which rosuvastatin attenuates cardiovascular remodelling in DOCA-salt animals is beyond the scope of this study. However, in addition to cholesterol reduction, HMG-CoA reductase inhibition also decreases mevalonate synthesis leading to changes in isoprenoid metabolism [43]. Because isoprenoid intermediates are important factors for the post-translational modification, maturation and membrane translocation of various regulatory proteins, such as the low molecular weight GTP-binding proteins of the Ras superfamily [44], it is possible that rosuvastatin-induced attenuation of cardiovascular remodelling is mediated by modifying the downstream products of cholesterol and, hence, mevalonate metabolism. In support of this, statins have been used to establish the functional involvement of the mevalonate pathway and these G-proteins in the regulation of cardiac myocyte [45], fibroblast [46] and vascular smooth muscle cell [47] mitogenesis. Furthermore, data suggests that Ras upregulation contributes to the development of DOCA-salt hypertension and associated reno-vascular hypertrophy and interstitial fibrosis [48] and this G-protein has also been implicated in the mineralocorticoid-induced mitogenesis of fibroblasts [49].

An elevated total cholesterol concentration has been demonstrated previously with DOCA-salt treatment in rats [50], and our results confirm this. The exact mechanism behind this elevation is unclear, but HMG-CoA inhibition by rosuvastatin normalized plasma levels in our rats, suggesting increased endogenous cholesterol synthesis. Whether these raised cholesterol levels and their subsequent abrogation by rosuvastatin had any effect on cardiovascular remodelling in this model is unlikely, but cannot be ruled out.

## **CONCLUSION**

In conclusion, we show for the first time that rosuvastatin attenuates cardiovascular remodelling, especially aortic medial thickening, myocardial inflammation and fibrosis, left ventricular hypertrophy and action potential prolongation, in DOCA-salt hypertensive rats without lowering blood pressure. These findings indicate the pleiotropic effects of the statins in rats that could explain, at least in part, improvements in survival and quality of life observed in patients treated with statins. Furthermore, the actions of rosuvastatin on cardiac remodelling may represent potential applications of statins beyond lipid lowering and atherosclerosis prevention or regression. Future studies using a therapeutic approach, that is a reversal protocol by commencing treatment after the onset of disease, are necessary to show the clinical relevance of these findings.

## **ACKNOWLEDGEMENTS**

This study was supported in part by a grant from AstraZeneca, Macclesfield, Cheshire U.K.

## REFERENCES

1. Sacks FM, Pfeffer MA, Moye LA, et al. The effect of pravastatin on coronary events after myocardial infarction in patients with average cholesterol levels. Cholesterol and Recurrent Events Trial investigators. *N Engl J Med* 1996;335:1001-1009.
2. Shepherd J, Cobbe SM, Ford I, et al. Prevention of coronary heart disease with pravastatin in men with hypercholesterolemia. West of Scotland Coronary Prevention Study Group. *N Engl J Med* 1995;333:1301-1307.
3. Downs JR, Clearfield M, Weis S, et al. Primary prevention of acute coronary events with lovastatin in men and women with average cholesterol levels: results of AFCAPS/TexCAPS. Air Force/Texas Coronary Atherosclerosis Prevention Study. *Jama* 1998;279:1615-1622.
4. Randomised trial of cholesterol lowering in 4444 patients with coronary heart disease: the Scandinavian Simvastatin Survival Study (4S). *Lancet* 1994;344:1383-1389.
5. Prevention of cardiovascular events and death with pravastatin in patients with coronary heart disease and a broad range of initial cholesterol levels. The Long-Term Intervention with Pravastatin in Ischaemic Disease (LIPID) Study Group. *N Engl J Med* 1998;339:1349-1357.
6. MRC/BHF Heart Protection Study of cholesterol lowering with simvastatin in 20,536 high-risk individuals: a randomised placebo-controlled trial. *Lancet* 2002;360:7-22.
7. Effect of simvastatin on coronary atheroma: the Multicentre Anti-Atheroma Study (MAAS). *Lancet* 1994;344:633-638.
8. Buchwald H, Campos CT, Boen JR, et al. Disease-free intervals after partial ileal bypass in patients with coronary heart disease and hypercholesterolemia: report from the Program on the Surgical Control of the Hyperlipidemias (POSCH). *J Am Coll Cardiol* 1995;26:351-357.
9. Liao JK, Laufs U. Pleiotropic effects of statins. *Annu Rev Pharmacol Toxicol* 2005;45:89-118.
10. Bauersachs J, Galuppo P, Fraccarollo D, et al. Improvement of left ventricular remodeling and function by hydroxymethylglutaryl coenzyme a reductase inhibition with cerivastatin in rats with heart failure after myocardial infarction. *Circulation* 2001;104:982-985.
11. Yu Y, Ohmori K, Chen Y, et al. Effects of pravastatin on progression of glucose intolerance and cardiovascular remodeling in a type II diabetes model. *J Am Coll Cardiol* 2004;44:904-913.
12. Serajuddin AT, Ranadive SA, Mahoney EM. Relative lipophilicities, solubilities, and structure-pharmacological considerations of 3-hydroxy-3-methylglutaryl-coenzyme A (HMG-CoA) reductase inhibitors pravastatin, lovastatin, mevastatin, and simvastatin. *J Pharm Sci* 1991;80:830-834.

13. McTaggart F, Buckett L, Davidson R, et al. Preclinical and clinical pharmacology of Rosuvastatin, a new 3-hydroxy-3-methylglutaryl coenzyme A reductase inhibitor. *Am J Cardiol* 2001;87:28B-32B.
14. Corsini A, Mazzotti M, Raiteri M, et al. Relationship between mevalonate pathway and arterial myocyte proliferation: in vitro studies with inhibitors of HMG-CoA reductase. *Atherosclerosis* 1993;101:117-125.
15. Oi S, Haneda T, Osaki J, et al. Lovastatin prevents angiotensin II-induced cardiac hypertrophy in cultured neonatal rat heart cells. *Eur J Pharmacol* 1999;376:139-148.
16. Bezerra DG, Mandarim-de-Lacerda CA. Beneficial effect of simvastatin and pravastatin treatment on adverse cardiac remodelling and glomeruli loss in spontaneously hypertensive rats. *Clin Sci (Lond)* 2005;108:349-355.
17. Jones PH, Davidson MH, Stein EA, et al. Comparison of the efficacy and safety of rosuvastatin versus atorvastatin, simvastatin, and pravastatin across doses (STELLAR\* Trial). *Am J Cardiol* 2003;92:152-160.
18. Di Napoli P, Taccardi AA, Grilli A, et al. Chronic treatment with rosuvastatin modulates nitric oxide synthase expression and reduces ischemia-reperfusion injury in rat hearts. *Cardiovasc Res* 2005;66:462-471.
19. Ikeda Y, Young LH, Lefer AM. Rosuvastatin, a new HMG-CoA reductase inhibitor, protects ischemic reperfused myocardium in normocholesterolemic rats. *J Cardiovasc Pharmacol* 2003;41:649-656.
20. Jones SP, Gibson MF, Rimmer DM, 3rd, et al. Direct vascular and cardioprotective effects of rosuvastatin, a new HMG-CoA reductase inhibitor. *J Am Coll Cardiol* 2002;40:1172-1178.
21. Brown L, Duce B, Miric G, et al. Reversal of cardiac fibrosis in deoxycorticosterone acetate-salt hypertensive rats by inhibition of the renin-angiotensin system. *J Am Soc Nephrol* 1999;10 Suppl 11:S143-148.
22. Miric G, Dallemagne C, Endre Z, et al. Reversal of cardiac and renal fibrosis by pirfenidone and spironolactone in streptozotocin-diabetic rats. *Br J Pharmacol* 2001;133:687-694.
23. Stegemann H, Stalder K. Determination of hydroxyproline. *Clin Chim Acta* 1967;18:267-273.
24. Ammarguella FZ, Gannon PO, Amiri F, et al. Fibrosis, matrix metalloproteinases, and inflammation in the heart of DOCA-salt hypertensive rats: role of ET(A) receptors. *Hypertension* 2002;39:679-684.
25. Endo A, Tsujita Y, Kuroda M, et al. Effects of ML-236B on cholesterol metabolism in mice and rats: lack of hypocholesterolemic activity in normal animals. *Biochim Biophys Acta* 1979;575:266-276.
26. Glorioso N, Troffa C, Filigheddu F, et al. Effect of the HMG-CoA reductase inhibitors on blood pressure in patients with essential hypertension and primary hypercholesterolemia. *Hypertension* 1999;34:1281-1286.
27. Delbosc S, Cristol JP, Descomps B, et al. Simvastatin prevents angiotensin II-induced cardiac alteration and oxidative stress. *Hypertension* 2002;40:142-147.
28. Jiang J, Roman RJ. Lovastatin prevents development of hypertension in spontaneously hypertensive rats. *Hypertension* 1997;30:968-974.

29. Gross V, Schneider W, Schunck WH, et al. Chronic effects of lovastatin and bezafibrate on cortical and medullary hemodynamics in deoxycorticosterone acetate-salt hypertensive mice. *J Am Soc Nephrol* 1999;10:1430-1439.
30. Ledingham JM, Laverty R. Fluvastatin remodels resistance arteries in genetically hypertensive rats, even in the absence of any effect on blood pressure. *Clin Exp Pharmacol Physiol* 2002;29:931-934.
31. Luo JD, Zhang WW, Zhang GP, et al. Simvastatin inhibits cardiac hypertrophy and angiotensin-converting enzyme activity in rats with aortic stenosis. *Clin Exp Pharmacol Physiol* 1999;26:903-908.
32. Kagitani S, Ueno H, Hirade S, et al. Tranilast attenuates myocardial fibrosis in association with suppression of monocyte/macrophage infiltration in DOCA/salt hypertensive rats. *J Hypertens* 2004;22:1007-1015.
33. Stalker TJ, Lefer AM, Scalia R. A new HMG-CoA reductase inhibitor, rosuvastatin, exerts anti-inflammatory effects on the microvascular endothelium: the role of mevalonic acid. *Br J Pharmacol* 2001;133:406-412.
34. Weber KT. From inflammation to fibrosis: a stiff stretch of highway. *Hypertension* 2004;43:716-719.
35. Fenning A, Harrison G, Rose'meyer R, et al. L-arginine attenuates cardiovascular impairment in DOCA-salt hypertensive rats. *Am J Physiol Heart Circ Physiol* 2005;
36. Allan A, Fenning A, Levick S, et al. Reversal of cardiac dysfunction by selective ET-A receptor antagonism. *Br J Pharmacol* 2005;(in press)
37. Tomaselli GF, Marban E. Electrophysiological remodeling in hypertrophy and heart failure. *Cardiovasc Res* 1999;42:270-283.
38. Coulombe A, Momtaz A, Richer P, et al. Reduction of calcium-independent transient outward potassium current density in DOCA salt hypertrophied rat ventricular myocytes. *Pflugers Arch* 1994;427:47-55.
39. Vogel RA. Coronary risk factors, endothelial function, and atherosclerosis: a review. *Clin Cardiol* 1997;20:426-432.
40. Egashira K, Hirooka Y, Kai H, et al. Reduction in serum cholesterol with pravastatin improves endothelium-dependent coronary vasomotion in patients with hypercholesterolemia. *Circulation* 1994;89:2519-2524.
41. O'Driscoll G, Green D, Taylor RR. Simvastatin, an HMG-coenzyme A reductase inhibitor, improves endothelial function within 1 month. *Circulation* 1997;95:1126-1131.
42. Treasure CB, Klein JL, Weintraub WS, et al. Beneficial effects of cholesterol-lowering therapy on the coronary endothelium in patients with coronary artery disease. *N Engl J Med* 1995;332:481-487.
43. Goldstein JL, Brown MS. Regulation of the mevalonate pathway. *Nature* 1990;343:425-430.
44. Magee T, Marshall C. New insights into the interaction of Ras with the plasma membrane. *Cell* 1999;98:9-12.
45. Takemoto M, Node K, Nakagami H, et al. Statins as antioxidant therapy for preventing cardiac myocyte hypertrophy. *J Clin Invest* 2001;108:1429-1437.

46. Porter KE, Turner NA, O'Regan DJ, et al. Simvastatin reduces human atrial myofibroblast proliferation independently of cholesterol lowering via inhibition of RhoA. *Cardiovasc Res* 2004;61:745-755.
47. Laufs U, Marra D, Node K, et al. 3-Hydroxy-3-methylglutaryl-CoA reductase inhibitors attenuate vascular smooth muscle proliferation by preventing rho GTPase-induced down-regulation of p27(Kip1). *J Biol Chem* 1999;274:21926-21931.
48. Muthalif MM, Benter IF, Khandekar Z, et al. Contribution of Ras GTPase/MAP kinase and cytochrome P450 metabolites to deoxycorticosterone-salt-induced hypertension. *Hypertension* 2000;35:457-463.
49. Stockand JD, Meszaros JG. Aldosterone stimulates proliferation of cardiac fibroblasts by activating Ki-RasA and MAPK1/2 signaling. *Am J Physiol Heart Circ Physiol* 2003;284:H176-184.
50. Hernandez N, Torres SH, De Sanctis JB, et al. Metabolic changes in DOCA-salt hypertensive rats. *Res Commun Mol Pathol Pharmacol* 2000;108:201-211.

Table 1: Physiological parameters in UNX, DOCA-salt and RSV-treated rats.

DATA	UNX	UNX+RSV	DOCA-salt	DOCA-salt+RSV
Initial Body Weight (g)	314±3 (n=10)	316±3 (n=10)	316±4 (n=12)	317±3 (n=12)
Final Body Weight (g)	404±7 (n=10)	410±6 (n=10)	316±7* (n=12)	335±7* (n=12)
0 week Systolic Blood Pressure (mmHg)	123±6 (n=10)	121±4 (n=10)	126±5 (n=9)	118±4 (n=8)
2 week Systolic Blood Pressure (mmHg)	123±6 (n=10)	117±4 (n=10)	160±9* (n=9)	155±10* (n=8)
Final Systolic Blood Pressure (mmHg)	122±4 (n=10)	118±3 (n=10)	188±3* (n=9)	194±7* (n=8)
LV+septum Weight (mg/g)	1.86±0.04 (n=10)	1.92±0.04 (n=10)	3.07±0.14* (n=12)	2.68±0.10* <sup>#</sup> (n=10)
Plasma Cholesterol Concentration (mM/L)	2.0±0.1 (n=7)	1.8±0.1 (n=7)	5.1±0.5* (n=7)	1.9±0.3 <sup>#</sup> (n=7)
Plasma Na <sup>+</sup> Concentration (mM)	130.4±1.1 (n=10)	130.1±0.3 (n=10)	136.3±0.8 (n=10)	133.5±1.0 (n=10)
Plasma K <sup>+</sup> Concentration (mM)	4.2±0.3 (n=10)	4.0±0.2 (n=10)	2.2±0.1* (n=10)	2.1±0.3* (n=10)
Diastolic Stiffness Constant ( $\kappa$ )	21.4±0.4 (n=10)	21.9±0.4 (n=9)	24.9±0.4* (n=12)	21.5±0.5 <sup>#</sup> (n=7)
Aortic Media Thickness ( $\mu$ m)	84.1±1.4 (n=7)	82.5±1.6 (n=10)	114.8±4.8* (n=11)	100.8±4.0* <sup>#</sup> (n=7)
Aortic Hydroxyproline Content ( $\mu$ g/mg)	15.6±0.7 (n=9)	15.3±0.5 (n=9)	15.4±0.4 (n=10)	15.2±0.4 (n=10)

\*p<0.05 compared to UNX, <sup>#</sup>p<0.05 compared to DOCA-salt

Table 2: Cardiac electrophysiological parameters in UNX, DOCA-salt and RSV-treated rats.

DATA	UNX	UNX+RSV	DOCA-salt	DOCA-salt+RSV
Resting Membrane Potential (mV)	-76±4 (n=6)	-75±3 (n=6)	-68±2 (n=6)	-70±2 (n=7)
Action Potential Amplitude (mV)	97±2 (n=6)	92±3 (n=6)	93±2 (n=6)	89±2 (n=7)
APD <sub>20</sub> (ms)	8.7±0.3 (n=6)	6.9±0.3 (n=6)	18.2±2.7* (n=6)	14.4±2.1 (n=7)
APD <sub>50</sub> (ms)	18.9±0.9 (n=6)	17.0±0.9 (n=6)	47.7±5.1* (n=6)	35.6±4.0* (n=7)
APD <sub>90</sub> (ms)	46.0±1.0 (n=6)	51.4±3.9 (n=6)	114.4±2.9* (n=6)	95.2±3.1* <sup>#</sup> (n=7)

\*p<0.05 compared to UNX, <sup>#</sup>p<0.05 compared to DOCA-salt

APD<sub>20</sub>, APD<sub>50</sub> and APD<sub>90</sub> = Action potential duration at 20%, 50% and 90% of repolarization respectively

**FIGURE 1**

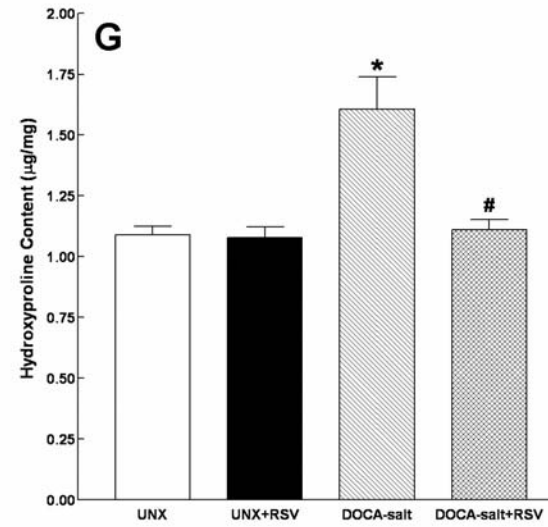
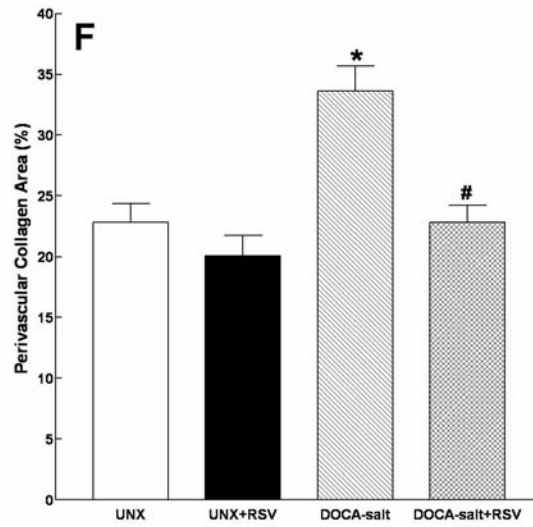
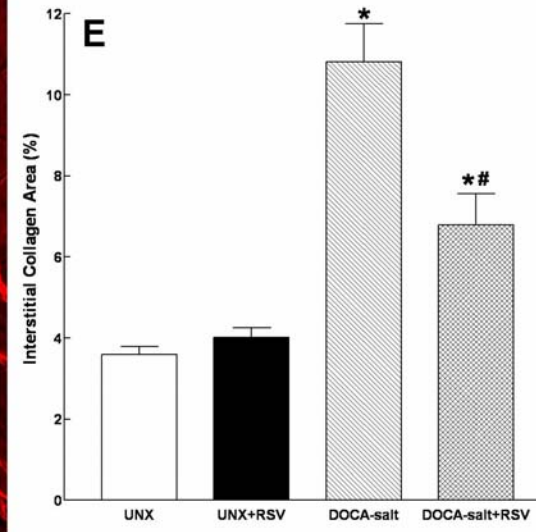
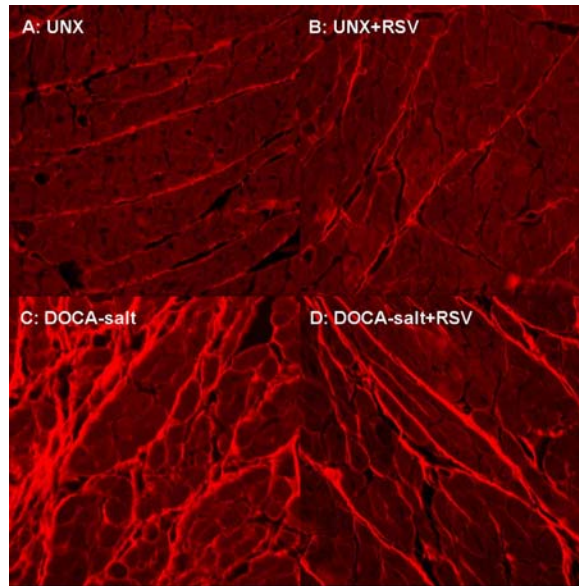


**FIGURE 2**

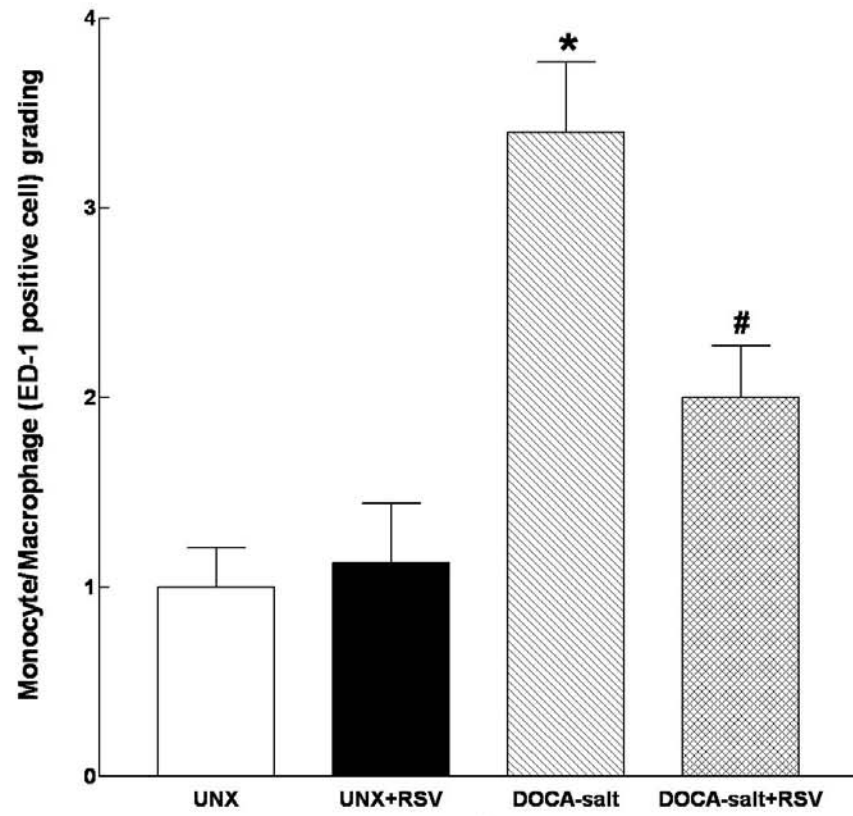
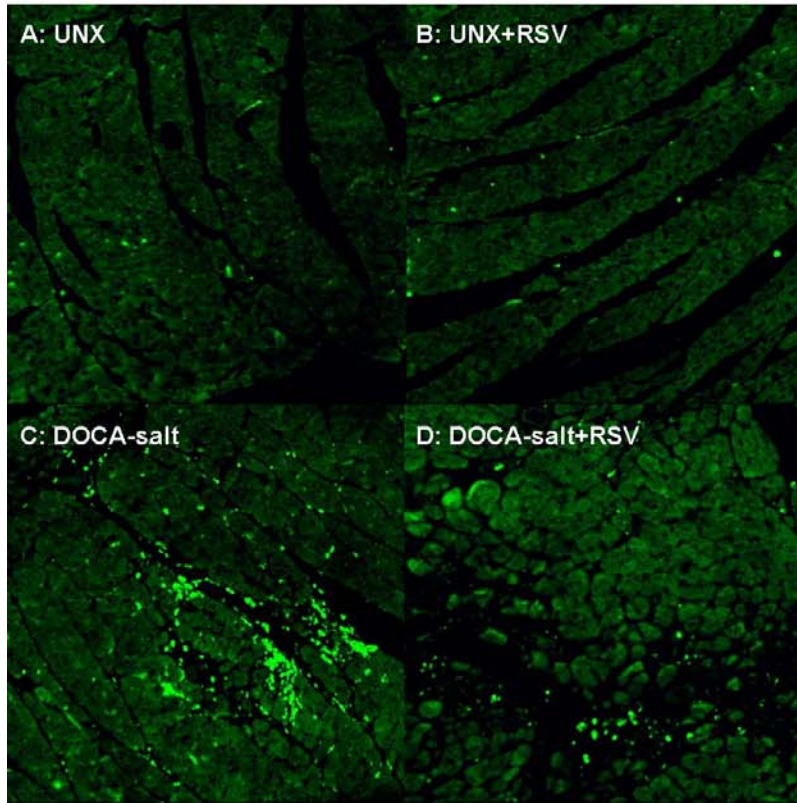


**FIGURE 3**

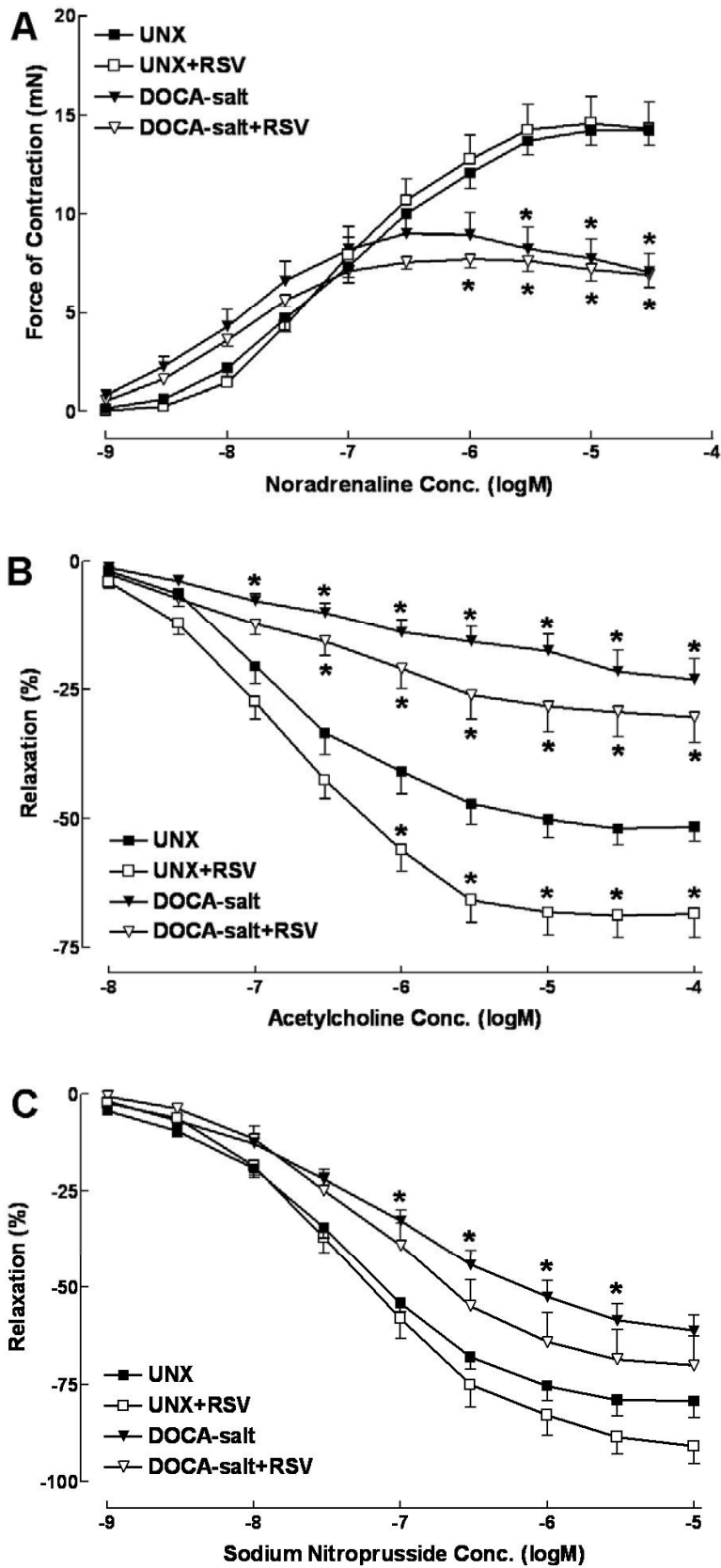


**FIGURE 4**

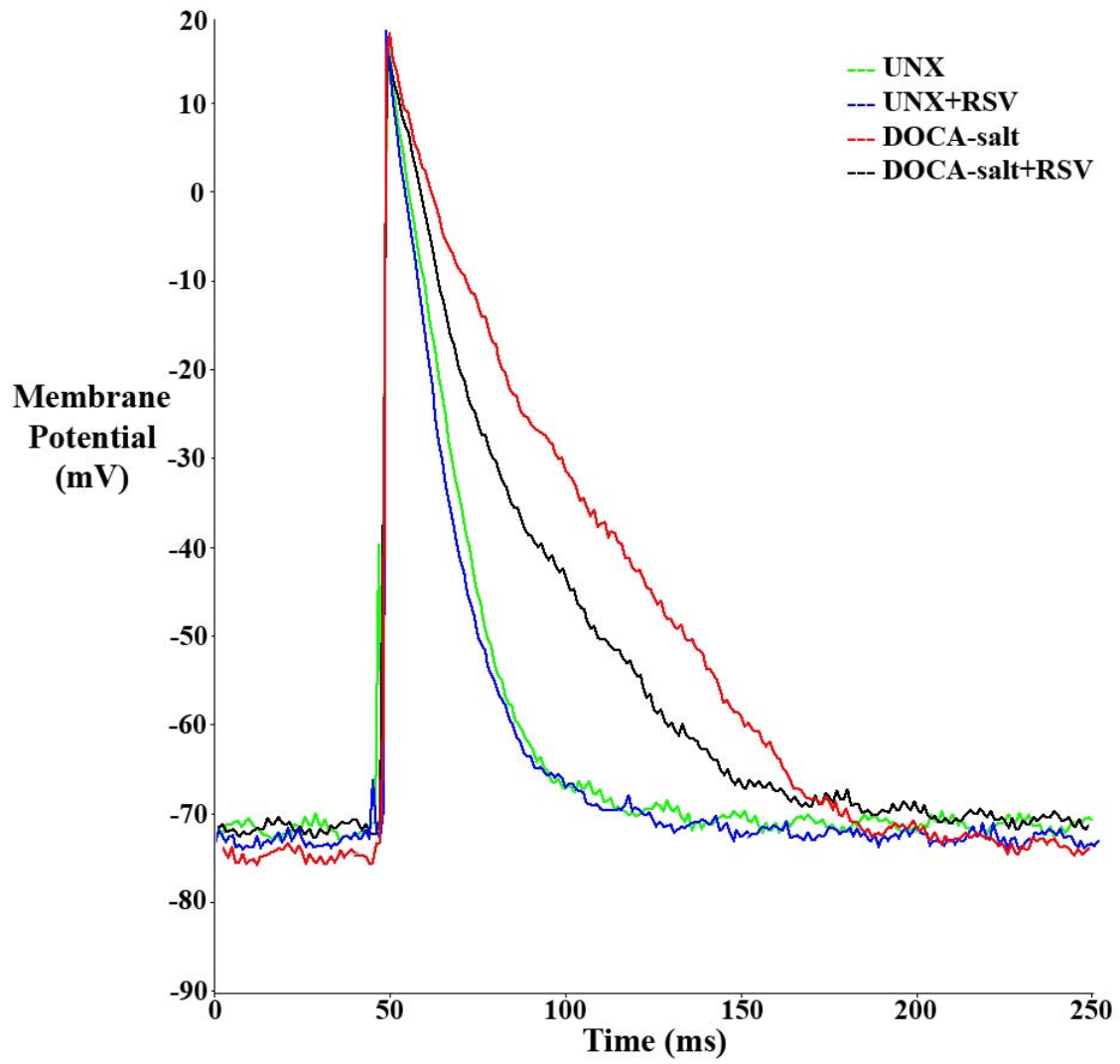


**FIGURE 1:** Representative picrosirius red stained confocal images of left ventricular interstitial collagen from UNX control (A), rosuvastatin-treated UNX (B), DOCA-salt control (C), and rosuvastatin-treated DOCA-salt (D) rats (magnification 40x). Graphical representations of left ventricular interstitial collagen area (E), perivascular collagen area (F) and hydroxyproline content (G). (\*  $p < 0.05$  vs UNX; #  $p < 0.05$  vs DOCA-salt).

**FIGURE 2:** Representative confocal images of left ventricular tissue showing immunofluorescent ED-1 positive monocyte/macrophages in UNX control (A), rosuvastatin-treated UNX (B), DOCA-salt control (C), and rosuvastatin-treated DOCA-salt (D) rats (magnification 20x). Graphical representation of ED-1 positive monocyte/macrophage left ventricular infiltration grading. (\*  $p < 0.05$  vs UNX; #  $p < 0.05$  vs DOCA-salt).

**FIGURE 3:** Concentration-response curves to noradrenaline (A) for UNX control (filled squares,  $-\log EC_{50} 7.0 \pm 0.1$ ,  $n=12$ ), rosuvastatin-treated UNX (open squares,  $-\log EC_{50} 7.1 \pm 0.1$ ,  $n=13$ ), DOCA-salt control (filled triangles,  $-\log EC_{50} 7.9 \pm 0.1^*$ ,  $n=11$ ) and rosuvastatin-treated DOCA-salt (open triangles,  $-\log EC_{50} 7.9 \pm 0.1^*$ ,  $n=11$ ) rats. Concentration-response curves to acetylcholine (B) for UNX control (filled squares,  $-\log EC_{50} 6.6 \pm 0.1$ ,  $n=11$ ), rosuvastatin-treated UNX (open squares,  $-\log EC_{50} 6.8 \pm 0.1$ ,  $n=12$ ), DOCA-salt control (filled triangles,  $-\log EC_{50} 6.5 \pm 0.1$ ,  $n=12$ ) and rosuvastatin-treated DOCA-salt (open triangles,  $-\log EC_{50} 6.6 \pm 0.1$ ,  $n=11$ ) rats. Concentration-response curves to sodium nitroprusside (C) for UNX control (filled squares,  $-\log EC_{50} 7.4 \pm 0.1$ ,  $n=12$ ), rosuvastatin-treated UNX (open squares,  $-\log EC_{50} 7.3 \pm 0.1$ ,  $n=13$ ), DOCA-salt control (filled triangles,  $-\log EC_{50} 7.1 \pm 0.1$ ,  $n=13$ ) and rosuvastatin-treated DOCA-salt (open triangles,  $-\log EC_{50} 7.1 \pm 0.1$ ,  $n=9$ ) rats. (\*  $p < 0.05$  vs UNX; #  $p < 0.05$  vs DOCA-salt).

**FIGURE 4:** Representative cardiac action potential recordings from UNX control (green), rosuvastatin-treated UNX (blue), DOCA-salt control (red) and rosuvastatin-treated DOCA-salt rats (black). Action potential prolongation can be observed in DOCA-salt controls and this can be attenuated by rosuvastatin treatment.